HAL
open science

Investigations on the thermo-mechanical behaviour of a complex assembly through dynamic mechanical analyses

Thibaut Vogel, Marion Girard, Pascal Casari, Jean-Christophe Walrick

To cite this version:

Thibaut Vogel, Marion Girard, Pascal Casari, Jean-Christophe Walrick. Investigations on the thermo-mechanical behaviour of a complex assembly through dynamic mechanical analyses. ICCS20 - 20th international conference on composite structures, Sep 2017, Paris, France. 10.15651/978-88-938-5041-4 . hal-04052775

HAL Id: hal-04052775

https://hal.science/hal-04052775v1

Submitted on 30 Mar 2023

HAL is a multi-disciplinary open access archive for the deposit and dissemination of scientific research documents, whether they are published or not. The documents may come from teaching and research institutions in France or abroad, or from public or private research centers.

L'archive ouverte pluridisciplinaire **HAL**, est destinée au dépôt et à la diffusion de documents scientifiques de niveau recherche, publiés ou non, émanant des établissements d'enseignement et de recherche français ou étrangers, des laboratoires publics ou privés.

Etude du comportement thermomécanique d'un assemblage complexe par essais dynamiques

Investigations on the thermo-mechanical behaviour of a complex assembly through dynamic mechanical analyses

Thibaut VOGEL[1], Marion GIRARD[2], Pascal CASARI[2], Jean-Christophe WALRICK[3],

1 : Mechanical Systems Design & Integration
Airbus Group Innovations
12 rue Pasteur, BP76, 92152 Suresnes Cedex, France
thibaut.vogel@airbus.com

2 : Institut de Recherche en Génie Civil et Mécanique, UMR CNRS 6183
Université de Nantes
58 rue Michel Ange, BP420, 44606 Saint-Nazaire Cedex, France
Marion.Girard@univ-nantes.fr ; Pascal.casari@univ-nantes.fr

3: ESTACA'LAB
ESTACA Campus Ouest
Parc Universitaire Laval-Changé, rue Georges Charpak, BP76121, Laval Cedex 9, France
jcwalrick@estaca.fr

1. Abstract

This work investigates the thermo-mechanical behaviour of sandwich structures where the skins are composed of glass/epoxy composite material, and the core consists of a structural epoxy adhesive. This type of structure is of particular interest to the aeronautical industry for the development of multifunctional structures such as composite structures integrating electrical components (conductors, antennas, batteries, super-capacitors, etc.) [1]–[4] which are embedded in the core of the sandwich. The design of such assemblies needs to ensure good interface properties to maintain optimal mechanical performances and electrical insulation of the embedded components during the lifespan of the structure [5], [6]. In particular, internal heating of the embedded components associated with the external thermal environment of an aeronautical structure is a sizing criteria for such structures [1]. Hence, it is necessary to characterize the thermo-mechanical behaviour of these assemblies in order to assess the good integrity of the interfaces and the stress field as a function of the temperature. In this study, the thermo-mechanical behaviour of a composite/epoxy adhesive/composite sandwich is characterized based on experimental data and numerical simulations. To start with, the temperature-dependence of the mechanical properties of the skins and the core are characterized through Dynamic Mechanical Analysis (DMA) testing. The temperature dependencies are then modelled with existing laws [7]–[13], and implemented in a non-linear Finite Element model. Finally, a comparison is made between DMA tests on various assemblies and their corresponding numerical models. The developed methodology allows the use of structural calculations to better characterize multi-layered sandwich structures under DMA testing. It also provides an efficient tool for the prediction of the thermo-mechanical behaviour of multi-layered and multi-material sandwich structures based on the thermo-mechanical behaviour of the constituents.

2. Theoretical Background

i. Experimental

The typical modulus versus temperature curve for a polymer exhibiting a secondary relaxation is shown by Figure 1. This temperature dependence is strongly related to molecular motions, and in particular to the inter- and intra-molecular bonds [14]. These bonds can be divided into two categories: primary bonds which consist in strong covalent intramolecular bonds and have a dissociation energy which varies between 50 and 200 kcal/mol, and secondary bonds such as hydrogen bonds, dipole interactions, Van der Waals interactions which can be dissociated much more easily (dissociation energy between 0.5 and 20 kcal/mol).

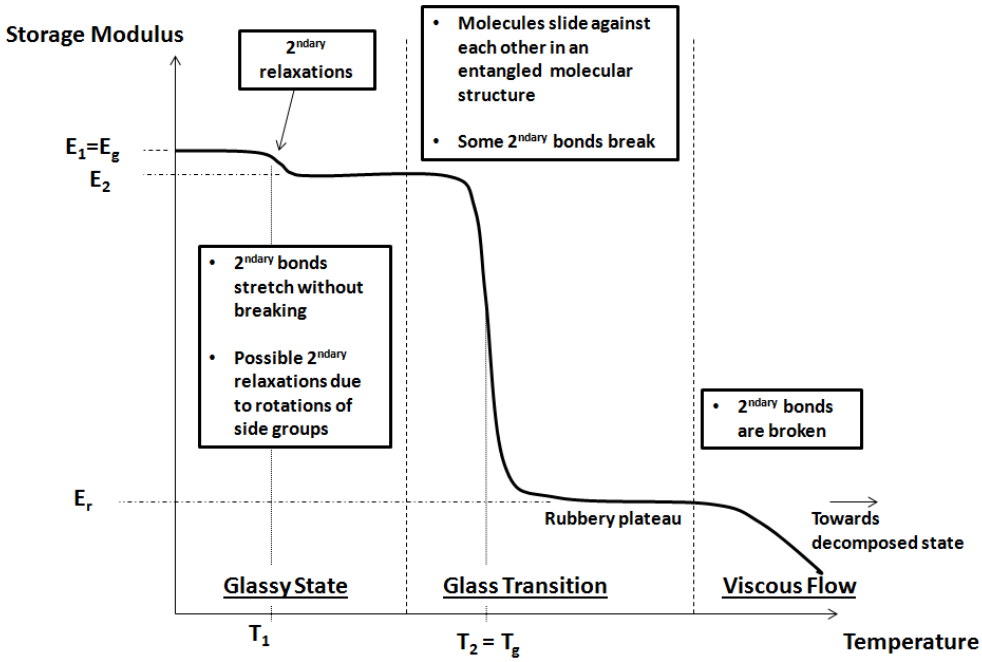

Figure 1 Modulus versus temperature for a typical polymer

In the lower temperature range the polymer is in the glassy state with intact primary and secondary bonds. As temperature increases, secondary bonds stretch without breaking resulting in a quasi-elastic behaviour of the polymer. In some cases secondary relaxations can occur if the thermal energy is high enough to allow rotation of side groups.
As the temperature is raised further, a much more noticeable relaxation occur, known as the alpha transition or the glass transition which results in a dramatic drop of the storage modulus until the rubbery plateau where the material state comprises intact primary bonds and broken secondary bonds.
At even higher temperature, the primary bonds are also broken and the material is decomposed which is noticeable by a new drop of the storage modulus (viscous flow).

ii. Modelling temperature-dependent mechanical properties

Modelling temperature-dependent mechanical properties of Fibre Reinforced Polymer (FRP) goes back to the 1980s, a complete review of such models has been done by Keller, et al. [8, 9]. Among the existing models, many consist in stepped functions connecting experimentally

gathered key points such as the glass transition temperature, and E-modulus values chosen in the various regions of the modulus versus temperature curve, cf. Figure 1.

Mahieux, et. Al [7], [8] defined a theoretical model for temperature-dependent E-modulus where they assumed a Weibull distribution to represent the process of bond rupture.

$$E = (E_1 - E_2).\exp\left(-\left(\frac{T}{T_1}\right)^{w_1}\right) + (E_2 - E_3).\exp\left(-\left(\frac{T}{T_2}\right)^{w_2}\right) + E_3.\exp\left(-\left(\frac{T}{T_3}\right)^{w_3}\right) \qquad \text{(Eq.1)}$$

where T is the temperature and E_i(i=1, 2, 3) represents the instantaneous stiffness of the material at the beginning of each plateau or state, as shown in Figure 1. The Weibull coefficients w_i corresponds to the statistics of bond breakage. This model successfully correlated experimental data conducted on six different polymers and will be used in this study.

Other models were developed, for instance by Bai, et al. [9] who modelled the temperature-dependent modulus using an Arrhenius-type equation. Gibson, et al. [10] who developed a semi-empirical model derived from phenomenological observations, allowing to describe the temperature-dependent modulus from the glass to the rubber state. And more recently, Feng and Guo [11], [12], [17] who added a physical meaning to Gibson's model by using the intrinsic growth rate of the number of rubber-state molecule per unit temperature [12]. Their consideration is based on a population growth model (logistic model). In addition, they defined a new parameter m which controls the symmetry of the glass transition region with respect to the glass transition temperature.

iii. Sandwich composite beam theory

According to the Timoshenko beam theory, the total maximum deflection Δ can be calculated as the sum of the deflections due to flexural and shear deformations (Δf and Δs respectively). For a dual cantilever beam, the equation can be written as follows [18]:

$$\Delta = \Delta_f + \Delta_s = \frac{FL^3}{24\langle EI\rangle} + \frac{FL}{2}\frac{k}{\langle GS\rangle} \qquad \text{(Eq.2)}$$

where F is the vertical load at midspan, L is half the distance between the supports, E and G are the elasticity and shear moduli, I the centroidal moment of inertia and S the cross-sectional area and k is a shear coefficient known as the shear area factor accounting for the fact that the shear stress distribution is not uniform through the thickness. The configuration is shown by Figure 2.

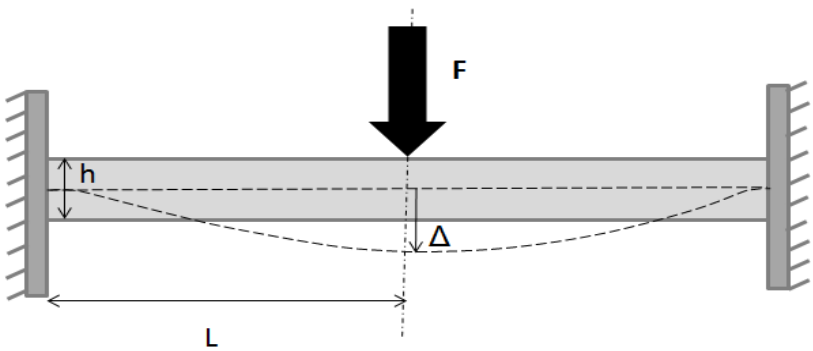

Figure 2 Dual cantilever configuration

In addition, it can be shown [18] that for a sandwich composite beam of width b, composed of two skins of thickness e_p with an elastic modulus E_p and shear modulus G_p, and a core of thickness e_c with an elastic modulus E_c and a shear modulus G_c:

$$\langle EI \rangle = E_p e_p b \frac{(e_c+e_p)^2}{2} + E_c \frac{e_c^3 b}{12} \qquad \text{(Eq.3)}$$

and

$$\langle GS \rangle = G_p e_p b + G_c e_c b \qquad \text{(Eq.4)}$$

For an isotropic material such as the epoxy adhesive, it can be assumed that:

$$G_c = \frac{E_c}{2(1+\vartheta_c)} \qquad \text{(Eq.5)}$$

with ϑ_c is the Poisson's ratio of the core material.

Besides, for an homogeneous rectangular cross section, the shear area factor k is usually chosen equal to 6/5. Yet, Gay [18] gives a more detailed expression when dealing with sandwich beam composites:

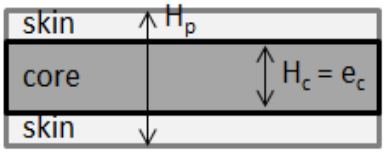

$$\begin{cases} k = \dfrac{a_k}{8\left[E_c H_c^3 + E_p(H_p^3 - H_c^3)\right]} expr_1 + expr_2 \\ expr_1 = \dfrac{E_c}{G_c} H_c^3 \left[E_p H_p^2 + (\dfrac{4}{5}E_c - E_p)H_c^2\right] + \dfrac{E_p^2}{G_p}(\dfrac{4}{5}H_p^5 + \dfrac{H_c^5}{5} - H_p^2 H_c^3) \\ expr_2 = \dfrac{3 b_k E_p (H_p^2 - H_c^2)}{E_c H_c^3 + E_p(H_p^3 - H_c^3)} \\ b_k = \dfrac{a_k}{16} H_c \dfrac{E_p}{G_p}\left\{\dfrac{H_c^2}{3} + H_p^2\left(\dfrac{G_p}{G_c} - 1\right) - H_c^2 \dfrac{G_p}{G_c}(1 - \dfrac{2}{3}\dfrac{E_c}{E_p})\right\} \end{cases} \qquad \text{(Eq.6)}$$

From (Eq.2) to (Eq.6) it is feasible to compute the temperature-dependent bending stiffness of a sandwich composite beam based on the stiffness temperature-dependence of the constituents.

3. Experiments

i. Procedure

The skins were made of an epoxy woven fabric composite with glass fabric reinforcement. Two lay-ups were analysed: $[0]_2$ and $[45]_2$. Additionally, a structural epoxy adhesive was used for the core.

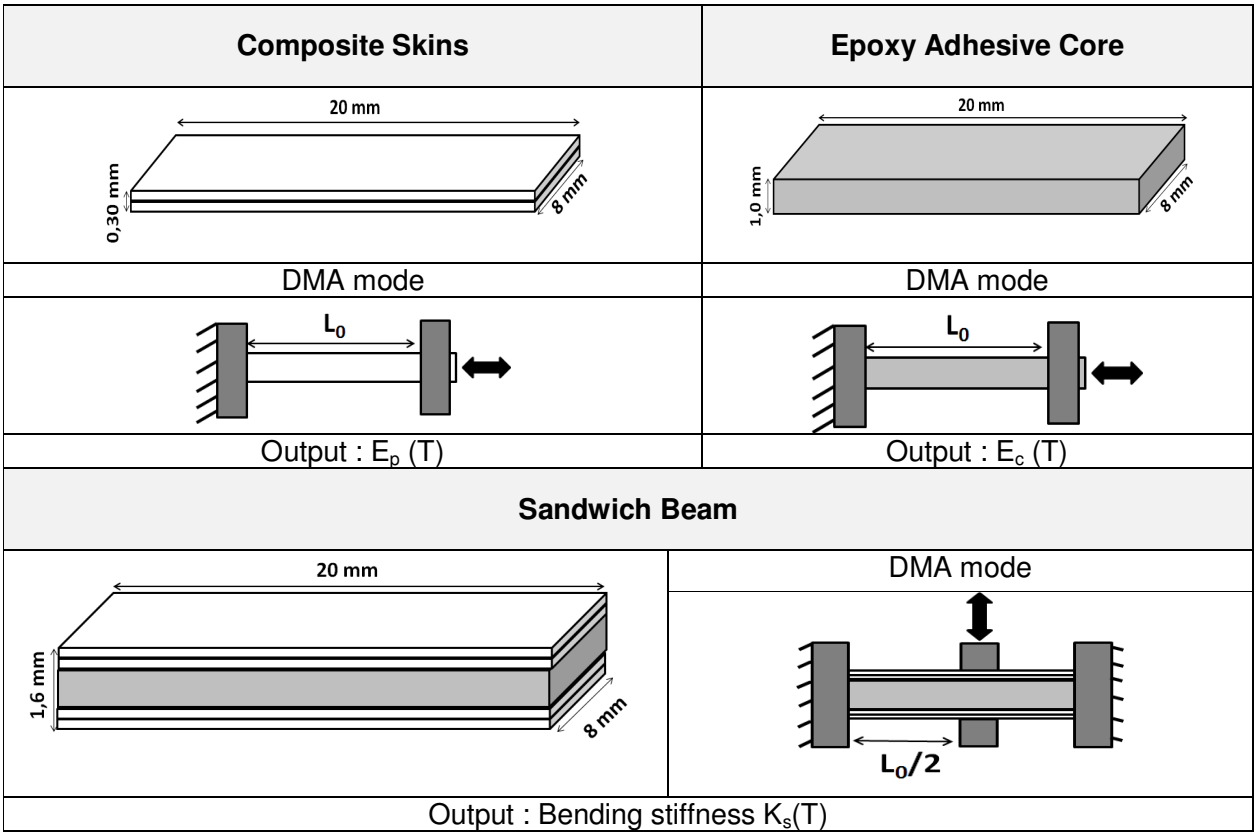

The composite skins were approximately 0,30mm thick (each ply is 0,15mm thick), and the epoxy adhesive was approximately 1,00mm thick. The sandwich test specimens were manufactured with either the 0° skins, or the 45° skins. Experiments were conducted on a TA Instruments DMA Q800 machine, using either the tensile mode (to characterize the constituent behaviour) or the double cantilever mode to characterize the sandwich beam, between 25°C and 200°C with a heating rate of 5°C/min at a frequency of 1Hz.

ii. Constituents

Figure 3 shows the evolution of the storage modulus of the three constituents plotted against temperature. Within the temperature range considered (25°C-150°C) the adhesive undergoes a complete glass transition. Indeed, the epoxy adhesive is in the glassy state at temperature below 310K with a stable storage modulus of about 3000MPa and in the rubber state at temperatures above 360K with a storage modulus of about 30MPa. The glass transition region starts from about 310K up to 360K with a glass transition temperature of approximately 340K.
The evolution of the storage modulus of the composite skins exhibits a different behaviour. There is no stable region for the storage modulus which decreases over a wide range of

temperature from room temperature (298K) to approximately 400K. When temperature is further increased the modulus drops more significantly, which corresponds to the glass transition temperature of the epoxy resin (420K according to manufacturer's datasheet).

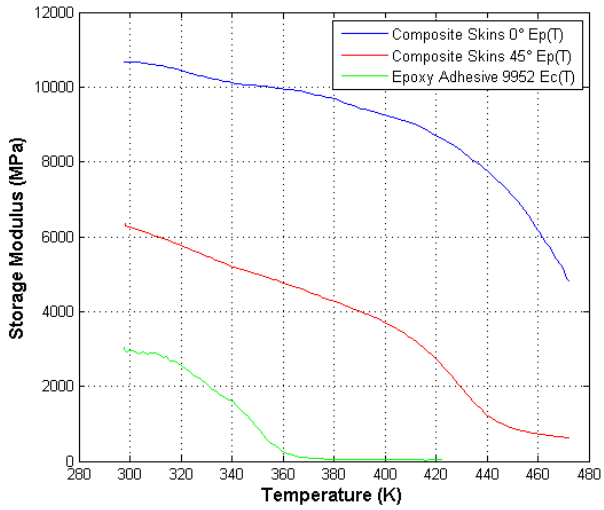

Figure 3 Storage modulus of the composite skins and epoxy structural adhesive under tensile mode

iii. *Sandwich beam*

The storage modulus of the sandwich test specimens exhibit a behaviour very similar to the epoxy adhesive, with a full transition observed near 350K. At room temperature, the stiffness of the sandwich with 0° skins is higher than the stiffness of the sandwich with 45° skins, hence indicating that at low temperature the bending stiffness is controlled by the skins. At higher temperature, a similar storage modulus is observed, which seems to indicate that beyond the glass transition, the bending behaviour is governed by the core material.

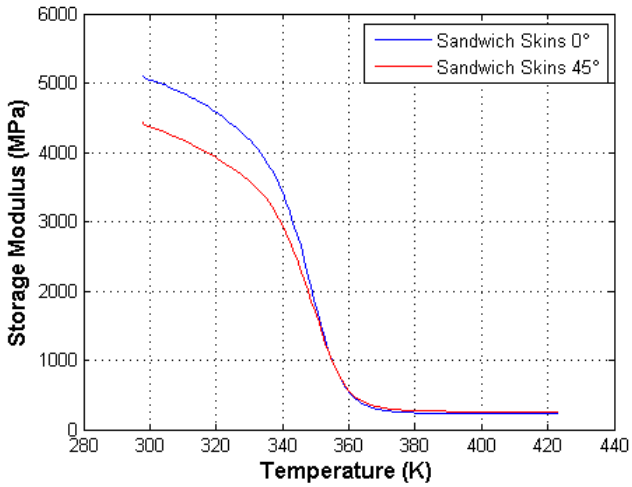

Figure 4 Storage modulus evolution of the sandwich samples under the dual cantilever mode

4. Numerical Modelling

The model of Mahieux [7], [8] discussed previously was used to model the temperature-dependent storage modulus of the constituents, cf. (Eq.1).

	E1	E2	E3	T1	T2	T3	w1	w2	w3
Comp45	8717	3000	502	345	430	450	4	35	20
Comp0	11055	9423	-	357	483,5	-	6,73	17,34	-
AXSON	3092	35	-	340	438	-	21,9	61,4	-

Table 1 Parameters used to fit the experimental data according to the model presented by Mahieux [8]

The parameters were determined with a non-linear least square fitting method. The evolution of the stiffness of the epoxy adhesive is modelled by taking into account a glass transition near 345K, and a decomposed state near 440K.

As regards to the composite skins for which the storage modulus exhibited a long and slow decrease with increasing temperature, a first transition is taken into account near 350K, and a second one (glass transition) near 430K for the 45° composite skins, and near 480K for the 0° composite skins. The decomposed state is taken into account only for the 45° skins with T_3 = 500K.

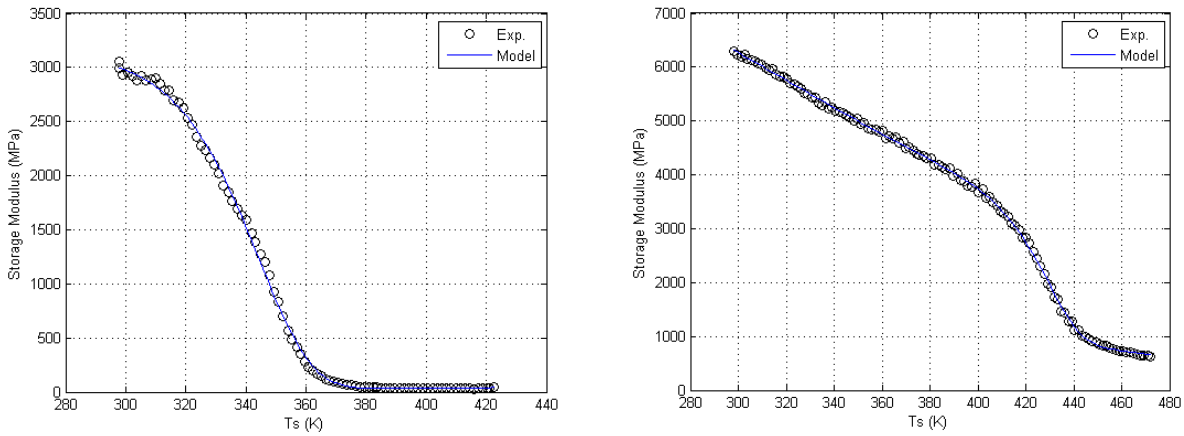

(a) (b)

Figure 5 Numerical fitting of the storage moduli of (a) the epoxy adhesive and (b) the 45° composite skins under tensile modes

5. Prediction of the temperature-dependent bending stiffness

i. Results

Under the dual cantilever mode, the storage modulus of a test sample is determined according to the equation below:

$$E' = \frac{K_S}{F_C}\frac{L^3}{24I}\left[1 + 2.\frac{6}{5}(1+v)\left(\frac{h}{L}\right)^2\right] \qquad \text{(Eq.7)}$$

With v the Poisson's ratio, L the sample length, h the sample thickness, I the sample moment of inertia, E the elastic modulus, K_s the measured stiffness and F_c a clamping correction factor. This expression assumes an isotropic homogeneous beam, hence it is likely that this expression is incorrect for the case considered here (sandwich composite beam). In particular, the second term of the expression is determined assuming a constant shear area factor (k=6/5) [19], whereas we have seen previously that this factor depends on the skins and core stiffness according to (Eq.6) which vary with the temperature.

In order to get rid of these correction factors, we focus on predicting the bending stiffness K_s of the sandwich beam which is experimentally determined as the ratio of the dynamic force by the dynamic displacement. This experimental stiffness is plotted in Figure 6 and compared with the numerical prediction determined by (Eq.2) with $K_s = F/\Delta$. A temperature-dependent shear area factor according to (Eq.6) is considered.

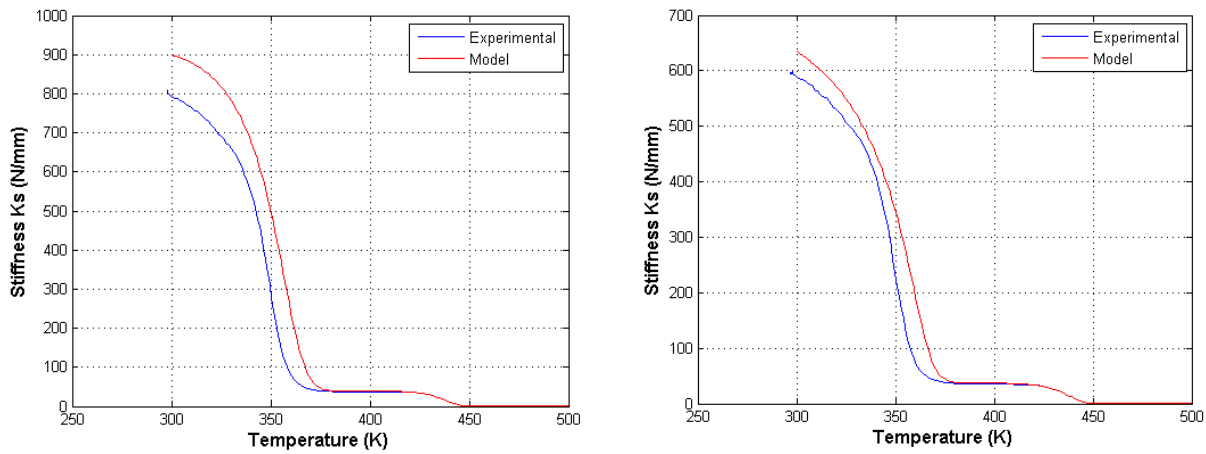

Figure 6 Prediction of the bending stiffness of the sandwich composite beam with elastic moduli equal to storage moduli with (a) 0° Composite skins and (b) 45° Composite skins

The temperature dependency of the bending stiffness correlates reasonably well with the experimental data. Yet, it can be seen that discrepancies exist in absolute values between the experimental and computed stiffness. Similar observations were made by Deng et al. [20] and Hobbiebrunken et al. [21] when they compared conventional mechanical testing data with DMA data, including in tension mode, cf. Figure 7. Similarly, Ropers, et al. [22] compared DMA data with the bending stiffness of thermoplastic composites and found good correlations on condition that proportionality factors are applied to the DMA data so that they match bending experiments. These discrepancies exist due to the instrumentation compliance, clamping and experimental conditions, test specimens dimensions, etc.

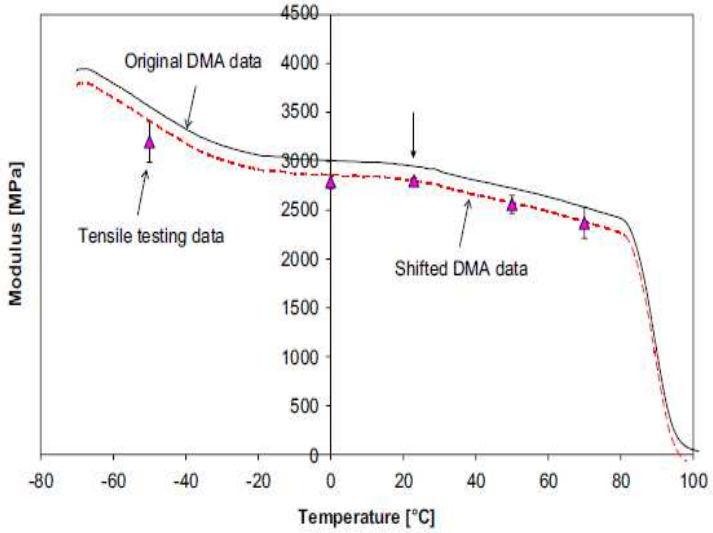

Figure 7 DMA data needs to be corrected to fit mechanical testing data in the work of Deng, et al. [20]

Therefore, it is likely that a proportionality factor needs to be applied to the storage modulus of the composite skins and epoxy adhesive to better represent the actual values of the elastic moduli. Hence, we choose to solve a nonlinear least-square curve-fitting so as to determine the proportionality factors α_p (with $E_p = \alpha_p E'_p$) and α_c (with $E_c = \alpha_c E'_c$) needed to match the numerical and experimental bending stiffness from Figure 6. The optimization returns $\alpha_p = 0.87$ and $\alpha_c = 0.93$. The new results are presented in Figure 8.

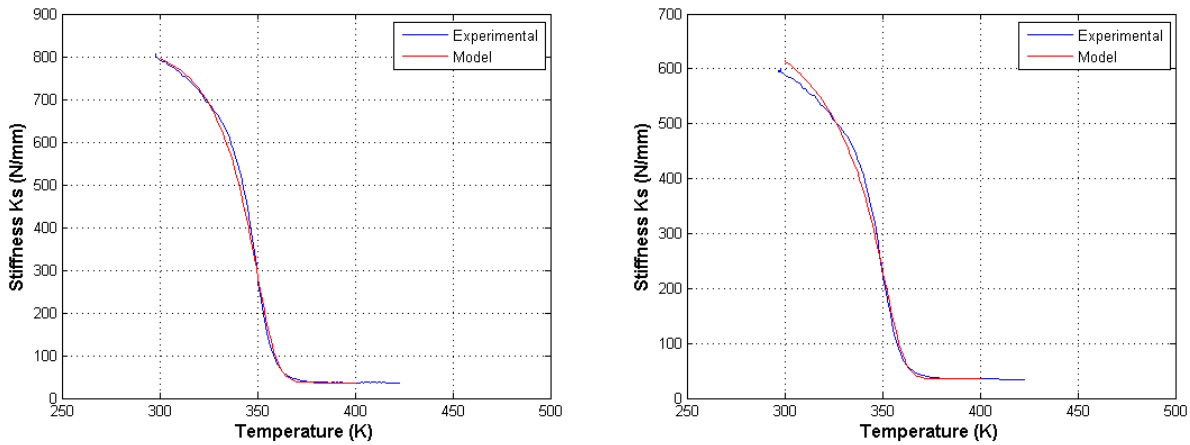

Figure 8 Prediction of the bending stiffness of the sandwich composite beam with shifted DMA data with(a) 0° Composite skins and (b) 45° Composite skins

With these small adjustments, the method allows computing the temperature-dependent bending stiffness of the sandwich assembly with a good correlation with experimental DMA data. It also justifies the use of the temperature dependency of the elastic moduli derived from the DMA to compute the bending stiffness.

ii. *Discussion on the shear correction factor*

It is interesting to notice that the temperature dependency of the shear area factor needs to be taken into account. Indeed, as shown by Figure 9, a constant shear area factor with a value of 6/5 poorly estimates the evolution of the bending stiffness. Numerically, we obtain that at room temperature k≈1,5 while at T = 100°C k≈37,2 and at T=170°C k≈187,6, cf. Figure 10.

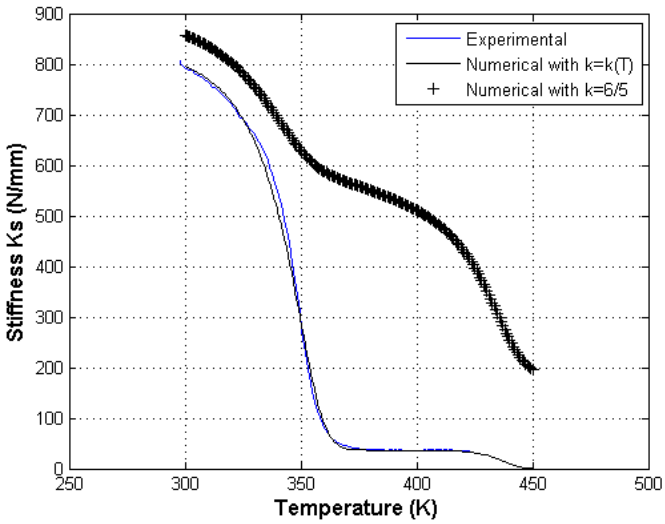

Figure 9 Prediction of the bending stiffness of the sandwich composite beam with a temperature dependent shear area factor

It underlines that the higher the temperature, the higher the contribution of the shear displacements to the total deflection of the sandwich beam since the deflection due to shear deformations is proportionally related to k (Eq.2). At temperatures higher than 450K, as E_c and G_c tends to zero, the shear area factor tends to infinity. As we had noticed, it is important to note that the storage modulus of such a multi-material assembly, determined by the DMA machine is most likely incorrect as (Eq.7) considers a constant value k=6/5.

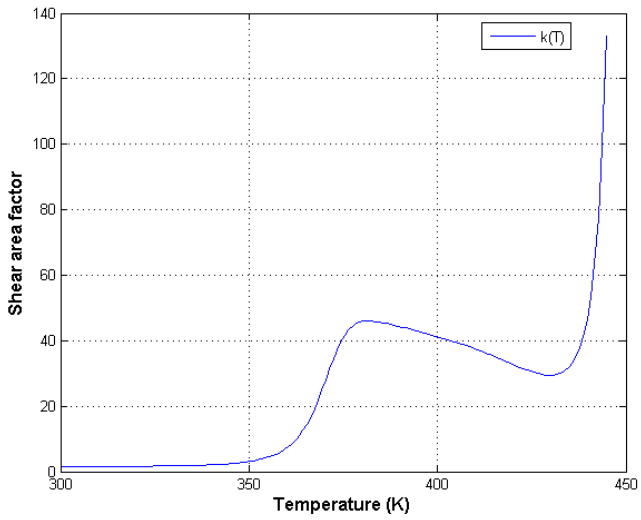

Figure 10 Evolution of the shear area factor with regards to temperature

Figure 11 plots the contribution of the flexural and shear deformations to the total deflection of the sandwich beam versus temperature. It further highlights that at temperatures higher than the glass transition temperature the deflection of the beam is governed by the shear deformations.

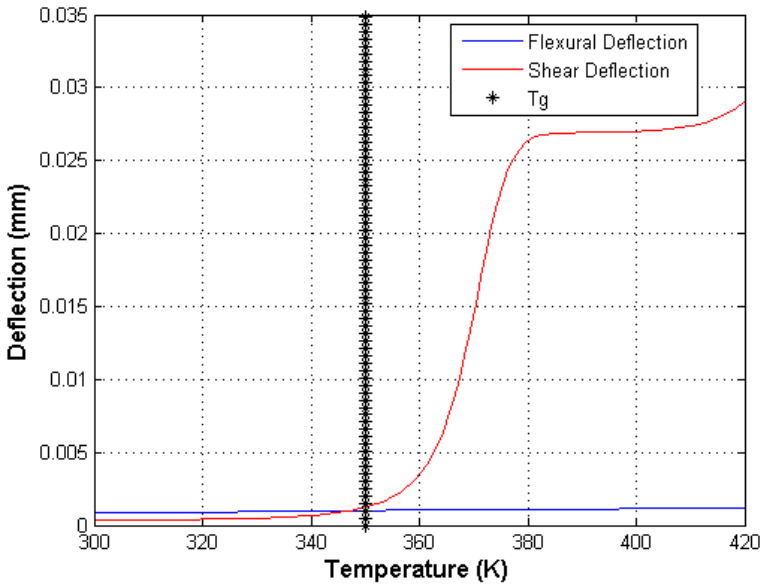

Figure 11 Flexural Δ_f and shear Δ_s deformations versus temperature

This change of behaviour at increasing temperature has particularly been noticed by Manalo et al. [23]. They observed that the flexural behaviour of a GFRP skin/phenolic core/GFRP skin sandwich system was governed by the GFRP skins up to 80°C (significant contribution to the sandwich stiffness and strength), and by the phenolic core beyond 80°C since the shear modulus of foam-core materials decreases at high temperature [24].

iii. Parameters sensitivity

A sensitivity study has been performed to investigate on the influence of the stiffness of the skins and core on the bending stiffness of the sandwich composite beam.

The system of equations (Eq.2) to (Eq.6) leading to the computation of the bending stiffness of the composite sandwich beam as a function of the dimensions of the test sample (ec, ep, b, L) and of the stiffness parameters (E_c, E_p, G_p) has been modelled with Artificial Neural Networks (ANN). Artificial neural networks consist in modelling complex nonlinear systems that are not easily modelled with a closed-form equation. Here, we want to quickly assess the influence of each parameter on the bending stiffness of the sandwich as a function of the temperature. The neural network is created with the Matlab's neural network toolbox.

Once the neural network has been created, it requires 7 inputs (e_c, e_p, b, L, E_c, E_p, G_p) and returns the bending stiffness of the sandwich composite beam as a function of temperature. The sensitivity of each parameter is then easily investigated. Figure 8 considers a variation of +/- 10% of each of the stiffness coefficients (E_c, E_p, G_p) taken separately and plots the absolute variation of the bending stiffness.

For instance, to investigate on the influence of E_p, a bending stiffness "$K_s_E_p$" is computed thanks to the neural network with several values of E_p taken within the range [0,90.E_p, 1,10.E_p]. The absolute variation of the bending stiffness is then computed according to (Eq.8).

$$Stiffness\ variation = \frac{K_s_E_p - K_s}{K_s} * 100 \qquad \text{(Eq.8)}$$

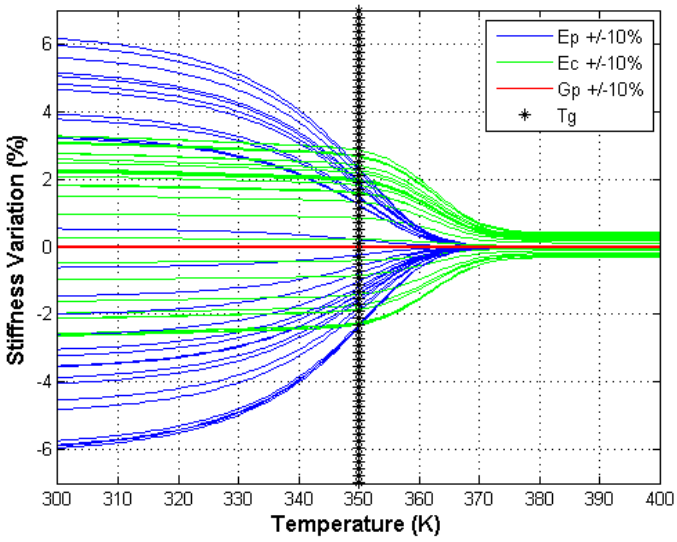

Figure 12 Variation of the bending stiffness of the sandwich beam with regards to a +/- 10% variation of the stiffness of the skins (E_p, G_p) and core (E_c)

Figure 12 underlines that at temperature lower than T_g, the stiffness of the skins has a predominant influence on the bending stiffness of the sandwich, while at temperature higher than T_g, the stiffness of the core plays a more influent role. The shear modulus of the skins G_p has barely any influence at all.

[Add the influence of the test specimen dimensions]

6. Finite Element Modelling

6.1. *Material Parameters*

This part aims at taking into account the stiffness-temperature dependencies of the composite skins and epoxy adhesive. A 3D FE model was developed to represent the DMA testing under the dual cantilever mode. Based on the results of the DMA tests under tensile mode on the composite skins and epoxy adhesive, each material properties is scaled according to Figure 13. The in-plane elastic moduli E_{11} and E_{22} are scaled according to the evolution of the storage modulus of the 0° composite skins under tensile mode. The shear moduli G_{12}, G_{13} and G_{23} are scaled according to the evolution of the storage modulus of the 45° composite skins under tensile mode. The out-of-plane elastic modulus E_{33} is approximated with the assumed thermo-mechanical behaviour of the epoxy resin with a glass transition temperature of 420K according to manufacturer's datasheet.

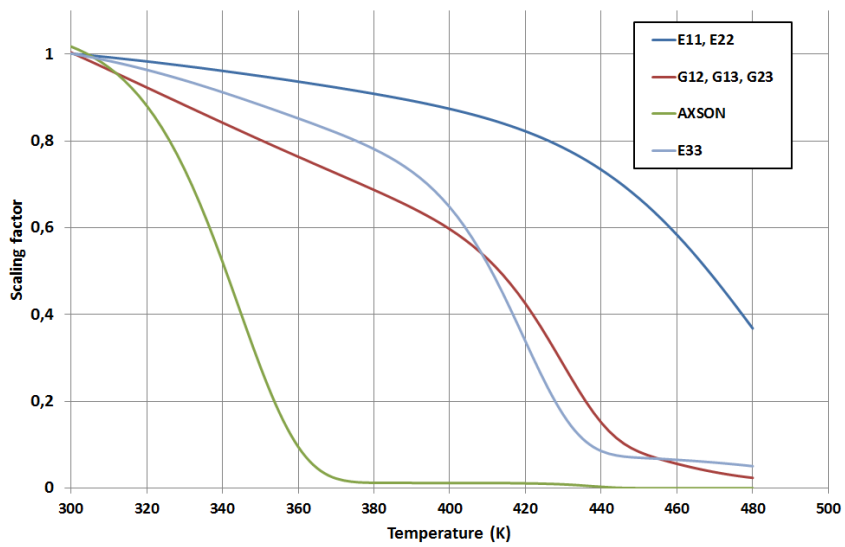

Figure 13 Scaling factors applied to the material properties as a function of temperature

6.2. *Model description*

The FE model is built with Abaqus CAE, the static and drive shafts are fully modelled as rigid bodies and the displacement of the mobile shaft is set to 4µm to model the experimental conditions. Tie constraints are applied between the upper and lower composite plies and the machine support.

Fully integrated linear isoparametric continuum elements are known to be too stiff in modelling flexural deformations of a beam. To overcome this shear-locking phenomenon, several possibilities exist: to use second-order isoparametric elements, incompatible mode elements, or reduced-integration elements with sufficiently through-the-thickness elements or with the enhanced hourglass control option [25].

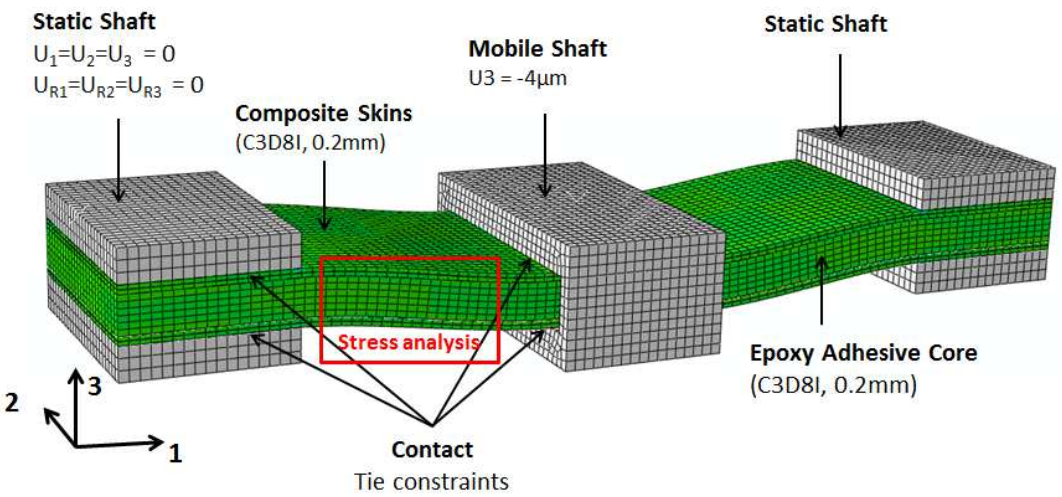

Figure 14 Finite Element Model of the Dual Cantilever Setup

Several elements are compared with various mesh size to assess the mesh convergence, cf. Figure 15. We choose to use C3D8I (incompatible mode eight-node brick elements) with a mesh size of 0.2mm with 6 elements through the thickness of the core and one element through the thickness of each composite ply. Quadratic elements with reduced integration (C3D20R) are expected to be more accurate but are much more costly than the linear elements with incompatible modes.

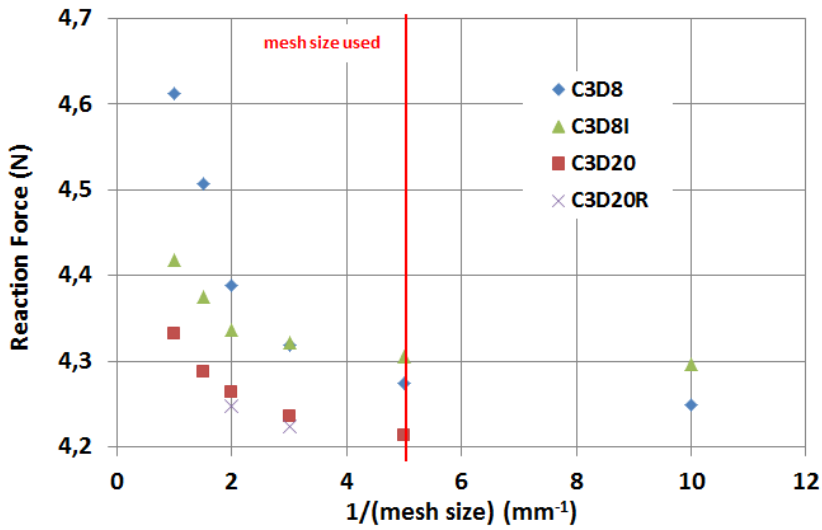

Figure 15 Mesh convergence as a function of the element types

6.3. Results

The first analysis consists in computing the bending stiffness of the test specimen at several temperatures. The results slightly over-predict the analytical and experimental bending stiffness, cf. Figure 16. This was expected as based on our mesh convergence study, our model tends to slightly over-predict the reaction force, hence the bending stiffness.

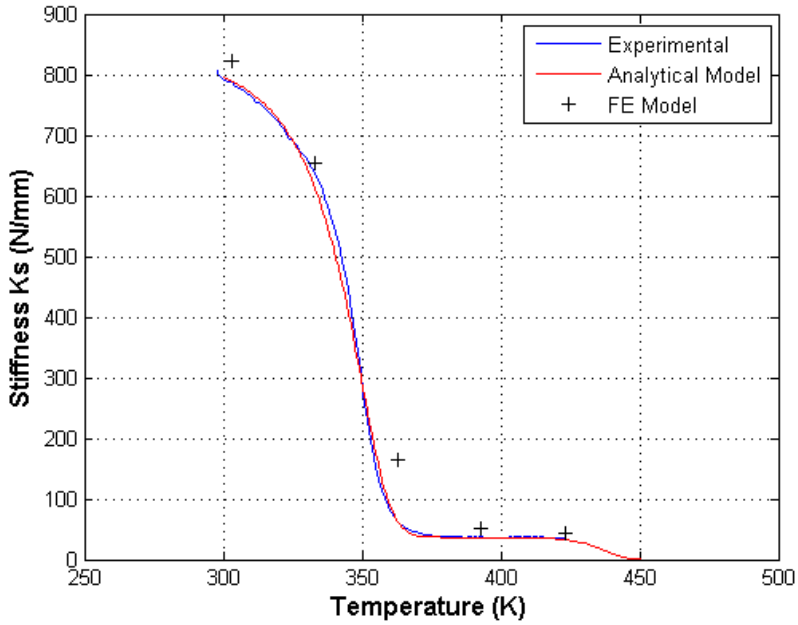

Figure 16 Comparison between Experimental DMA Data, Analytical Model and FE Model

The second analysis consists in analysing the longitudinal and inter-laminar stress in the middle of the sandwich beam. Hence, Figure 16 below plots the longitudinal stresses S_{11} and inter-laminar stresses S_{13} at mid-distance from each support, as shown in Figure 14.

Tempe -rature	S11 (MPa)	S13 (MPa)
30°C	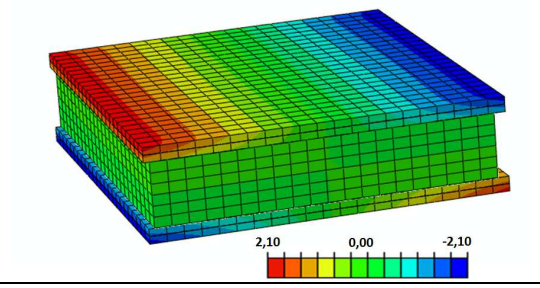	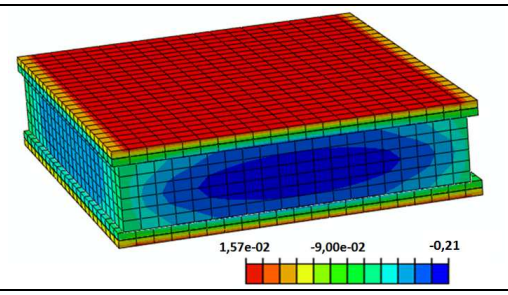
60°C	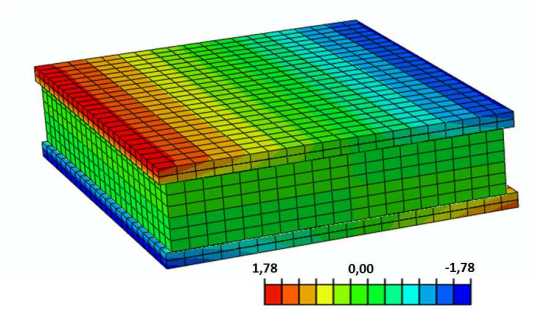	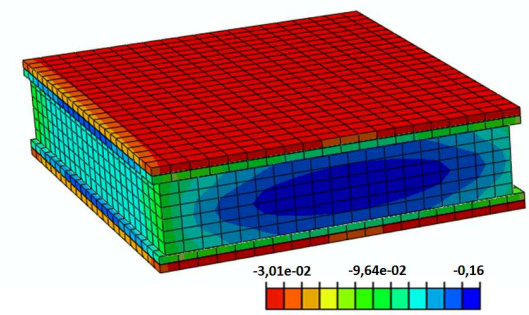

90°C	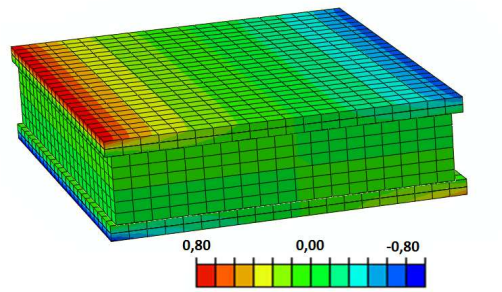	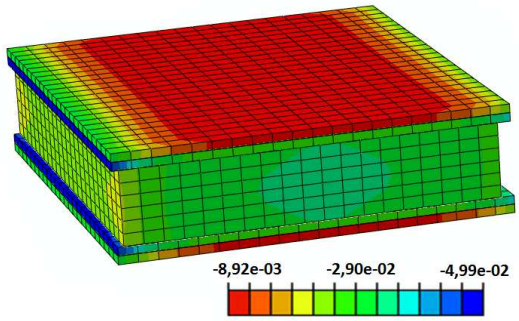
120°C	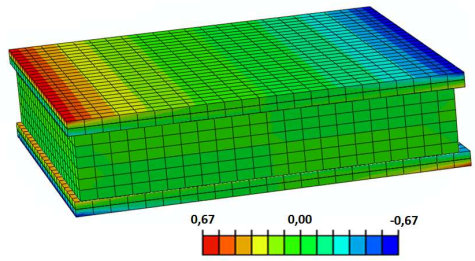	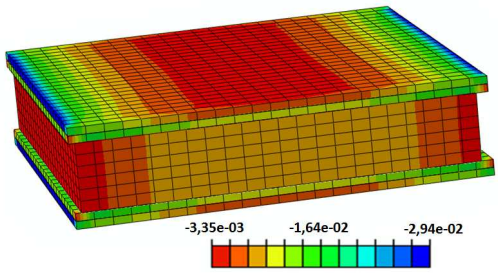
150°C	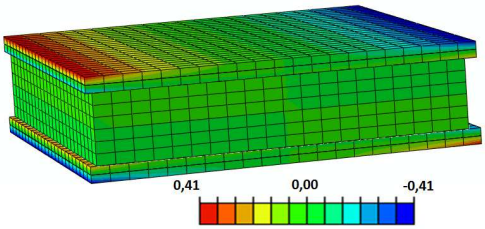	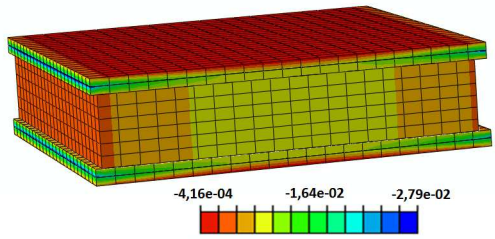

7. Conclusion

- Analytical prediction of the temperature-dependent bending stiffness of a sandwich assembly based on DMA data
- Numerical characterisation of the temperature-dependence of the shear correction factor
- USE of DMA data in a FE code to predict the bending stiffness and stress distribution within the sandwich assembly

1. References

[1] T. Seong Jang, D. Soo Oh, J. Kyu Kim, K. In Kang, W. Ho Cha, and S. Woo Rhee, 'Development of multi-functional composite structures with embedded electronics for space application', *Acta Astronaut.*, vol. 68, no. 1–2, pp. 240–252, Jan. 2011.

[2] R. F. Gibson, 'A review of recent research on mechanics of multifunctional composite materials and structures', *Compos. Struct.*, vol. 92, no. 12, pp. 2793–2810, Nov. 2010.

[3] M. S. Qidwai, J. Thomas, and W. Pogue, 'Structure-battery composites for UUVs: multifunctional interaction effects', in *50th AIAA/ASME/ASCE/AHS/ASC Structures, Structural Dynamics, and Materials Conference 17th AIAA/ASME/AHS Adaptive Structures Conference 11th AIAA No*, 2009, p. 2341.

[4] A. K. Noor, S. L. Venneri, D. B. Paul, and M. A. Hopkins, 'Structures technology for future aerospace systems', *Comput. Struct.*, vol. 74, no. 5, pp. 507–519, 2000.

[5] H. Kim and K. Hsieh, 'Measurement and prediction of embedded copper foil fatigue crack growth in multifunctional composite structure', *Compos. Part Appl. Sci. Manuf.*, vol. 43, no. 3, pp. 492–506, Mar. 2012.

[6] J.-C. Walrick, M. Grésil, and P. Parneix, 'Influence sur la tenue mécanique de l'insertion d'une fonction de protection électromagnétique au sein de composites à renforts de fibres de verre= Strength mechanical influence of electromagnetic shield function embedded in laminated glass composite', in *JNC 16*, 2009, p. 10–p.

[7] C. A. Mahieux and K. L. Reifsnider, 'Property modeling across transition temperatures in polymers: a robust stiffness–temperature model', *Polymer*, vol. 42, no. 7, pp. 3281–3291, 2001.

[8] C. A. Mahieux, 'A systematic stiffness-temperature model for polymers and applications to the prediction of composite behavior', Ph.D. Dissertation, Virginia Polytechnic Institute and State University, 1999.

[9] Y. Bai, T. Keller, and T. Vallée, 'Modeling of stiffness of FRP composiets under elevated and high temperatures', *Composites Science and Technology*, pp. 3099–3106, 2008.

[10] A. Gibson, T. Brownes, S. Feih, and A. Mouritz, 'Modeling composite high temperature behavior and fire response under load', *Journal of Composite Materials*, pp. 2005–2022, 2012.

[11] Z. Guo, J. Feng, H. Wang, H. Hu, and J. Zhang, 'A new temperature-dependent modulus model of glass/epoxy composite at elevated temperature', *J. Compos. Mater.*, vol. 47, no. 26, pp. 3303–3310, 2013.

[12] J. Feng, W. Hui, Z. Guo, H. Hu, and J. Zhang, 'Model for Temperature-dependence modulus of Glass/Epoxy Composite', presented at the Third International Conference on Smart Materials and Nanotechnology in Engineering, Shenzen, China, 2012, vol. 8409.

[13] J. Feng and Z. Guo, 'Temperature-frequency-dependent mechanical properties model of epoxy resin and its composites', *Composites Part B: Engineering*, pp. 161–169, Feb-2016.

[14] M. F. Ashby and D. R. H. Jones, *Engineering materials 2: An introduction to microstructures, processing and design*, 3. ed., Reprinted. Amsterdam: Elsevier, 2008.

[15] T. Keller, C. Tracy, and A. Zhou, 'Structural response of liquid-cooled GFRP slabs subjected to fire – Part I: Material and post-fire modeling', *Compos. Part Appl. Sci. Manuf.*, vol. 37, no. 9, pp. 1286–1295, Sep. 2006.

[16] T. Keller, C. Tracy, and A. Zhou, 'Structural response of liquid-cooled GFRP slabs subjected to fire – Part II: Thermo-chemical and thermo-mechanical modeling', *Compos. Part Appl. Sci. Manuf.*, vol. 37, no. 9, pp. 1296–1308, Sep. 2006.

[17] J. Feng and Z. Guo, 'Temperature-frequency-dependent mechanical properties of epoxy resin and its composites', *Compos. Part B Eng.*, vol. 85, pp. 161–169, 2016.

[18] D. Gay, *Matériaux Composites*, 5th ed. Paris: Lavoisier, 2005.

[19] H. Osnes and T. Thorvaldsen, 'Dynamic mechanical analysis–theoretical considerations on mechanical properties', *Nor. Def. Res. Establ. FFI-Rapp.*, vol. 1656, 2011.
[20] S. Deng, M. Hou, and L. Ye, 'Temperature-dependent elastic moduli of epoxies measured by DMA and their correlations to mechanical testing data', *Polym. Test.*, vol. 26, no. 6, pp. 803–813, Sep. 2007.
[21] T. Hobbiebrunken, B. Fiedler, M. Hojo, S. Ochiai, and K. Schulte, 'Microscopic yielding of CF/epoxy composites and the effect on the formation of thermal residual stresses', *Compos. Sci. Technol.*, vol. 65, no. 10, pp. 1626–1635, Aug. 2005.
[22] S. Ropers, M. Kardos, and T. A. Osswald, 'A thermo-viscoelastic approach for the characterization and modeling of the bending behavior of thermoplastic composites', *Compos. Part Appl. Sci. Manuf.*, vol. 90, pp. 22–32, Nov. 2016.
[23] A. Manalo, S. Surendar, G. van Erp, and B. Benmokrane, 'Flexural behavior of an FRP sandwich system with glass-fiber skins and a phenolic core at elevated in-service temperature', *Compos. Struct.*, vol. 152, pp. 96–105, Sep. 2016.
[24] S. Zhang, J. M. Dulieu-Barton, and O. T. Thomsen, 'The effect of temperature on the failure modes of polymer foam cored sandwich structures', *Compos. Struct.*, vol. 121, pp. 104–113, Mar. 2015.
[25] *ABAQUS (2011) 'Abaqus Documentation'*, Dassault Systèmes, Providence, RI, USA. .